

2-5-2021

Charge density wave and superconductivity in the disordered Holstein model

B. Xiao

University of California, Davis

N. C. Costa

Universidade Federal do Rio de Janeiro

E. Khatami

San Jose State University, ehsan.khatami@sjsu.edu

G. G. Batrouni

Université Côte d'Azur

R. T. Scalettar

University of California, Davis

Follow this and additional works at: https://scholarworks.sjsu.edu/faculty_rsca

Recommended Citation

B. Xiao, N. C. Costa, E. Khatami, G. G. Batrouni, and R. T. Scalettar. "Charge density wave and superconductivity in the disordered Holstein model" *Physical Review B* (2021). <https://doi.org/10.1103/PhysRevB.103.L060501>

This Article is brought to you for free and open access by SJSU ScholarWorks. It has been accepted for inclusion in Faculty Research, Scholarly, and Creative Activity by an authorized administrator of SJSU ScholarWorks. For more information, please contact scholarworks@sjsu.edu.

Charge density wave and superconductivity in the disordered Holstein model

B. Xiao^{1,2}, N. C. Costa^{3,4}, E. Khatami⁵, G. G. Batrouni^{6,7,8,9} and R. T. Scalettar¹

¹Department of Physics, University of California, Davis, California 95616, USA

²Center for Computational Quantum Physics, Flatiron Institute, New York, New York 10010, USA

³Instituto de Física, Universidade Federal do Rio de Janeiro Cx. P. 68.528, 21941-972 Rio de Janeiro, RJ, Brazil

⁴International School for Advanced Studies (SISSA), Via Bonomea 265, 34136 Trieste, Italy


⁵Department of Physics and Astronomy, San José State University, San José, California 95192, USA

⁶Université Côte d'Azur, CNRS, INPHYNI, 0600 Nice, France

⁷Centre for Quantum Technologies, National University of Singapore, 2 Science Drive 3, 117542 Singapore

⁸Department of Physics, National University of Singapore, 2 Science Drive 3, 117542 Singapore

⁹Beijing Computational Science Research Center, Beijing 100193, China

 (Received 27 October 2019; revised 31 August 2020; accepted 19 January 2021; published 5 February 2021)

The interplay between electron-electron correlations and disorder has been a central theme of condensed matter physics over the past several decades, with particular interest in the possibility that interactions might cause delocalization of an Anderson insulator into a metallic state, and the disrupting effects of randomness on magnetic order and the Mott phase. Here we extend this physics to explore *electron-phonon* interactions and show, via exact quantum Monte Carlo simulations, that the suppression of the charge density wave correlations in the half-filled Holstein model by disorder can stabilize a superconducting phase. Our simulations thus capture qualitatively the suppression of charge ordered phases and emergent superconductivity recently seen experimentally.

DOI: [10.1103/PhysRevB.103.L060501](https://doi.org/10.1103/PhysRevB.103.L060501)

Introduction. Although the problem of the localizing effect of randomness on *noninteracting* electrons is well understood [1–3], the combined effects of disorder and electron-electron interactions remain an area of continued theoretical and experimental interest [4–11]. A traditional focus has been on the possibility of electron-electron interactions inducing an insulator-to-metal transition in two dimensions [12], but recent attention has also turned to understanding the interplay in the context of modern developments including Majorana fermions [13], topological bands [14], ultracold atomic gases [15], and many-body localization [16–18]. Supplementing analytic calculations, numerical approaches have attempted to address the issue with techniques that treat disorder and electronic correlations nonperturbatively [19,20]. Unfortunately, in quantum Monte Carlo (QMC) methodologies, the combination of randomness and interactions often leads to the fermion minus-sign problem, a bottleneck that dramatically limits their effectiveness [21–23].

In this work, we use an exact sign-problem-free QMC approach to investigate the interplay between randomness and *electron-phonon interactions*. This is an area far less explored with numerical simulations than that of randomness and electron-electron interactions. This gives us the opportunity, within the framework of the disordered Holstein model, to address important fundamental qualitative issues. Among them, we find the emergence of a superconducting (SC) phase upon the suppression of the charge density wave (CDW) order by randomness. Further, the absence of the sign problem

allows us to reach low temperatures, and thus use the full power of QMC calculations, which cannot be fully exploited for electron-electron interactions.

This paper is organized as follows: After describing our Hamiltonian and methodology in the “Model” and “Methods” sections, we show in the “Results” section the details of the quantum simulations that lead to a demonstration of the emergence of a SC phase driven by the interplay of electron-phonon interaction and randomness. Our final remarks are in the “Concluding remarks” section. Further results about the magnitude of SC and CDW correlations in the full temperature-disorder plane are presented in the Supplemental Material (SM) [28].

Model. The Holstein model describes itinerant electrons whose site density couples to the displacement of a local phonon mode. Its Hamiltonian reads

$$\mathcal{H} = -t \sum_{\langle \mathbf{i}, \mathbf{j} \rangle, \sigma} (d_{\mathbf{i}\sigma}^\dagger d_{\mathbf{j}\sigma} + \text{H.c.}) - \sum_{\mathbf{i}, \sigma} (\mu - \epsilon_{\mathbf{i}}) n_{\mathbf{i}, \sigma} + \omega_0 \sum_{\mathbf{i}} a_{\mathbf{i}}^\dagger a_{\mathbf{i}} + g \sum_{\mathbf{i}, \sigma} n_{\mathbf{i}\sigma} (a_{\mathbf{i}}^\dagger + a_{\mathbf{i}}), \quad (1)$$

in which the sum over \mathbf{i} is on a two-dimensional square lattice, with $\langle \mathbf{i}, \mathbf{j} \rangle$ denoting nearest neighbors. $d_{\mathbf{i}\sigma}^\dagger$ ($d_{\mathbf{i}\sigma}$) is the creation (annihilation) operator of electrons with spin σ at site \mathbf{i} , with $n_{\mathbf{i}\sigma} \equiv d_{\mathbf{i}\sigma}^\dagger d_{\mathbf{i}\sigma}$ denoting the number operator. $a_{\mathbf{i}}^\dagger$ ($a_{\mathbf{i}}$) is the phonon creation (annihilation) operator. The first term on the right-hand side of Eq. (1) corresponds to the hopping of electrons, and the second term contains the global chemical

potential μ . Disorder effects are introduced in the second term by means of random on-site energies ϵ_i , chosen uniformly in the range $[-\Delta/2, \Delta/2]$, so that Δ/t represents the dimensionless disorder strength. Local phonon modes, with energy ω_0 , are included in the third term. Finally, the last term describes their coupling to electrons, with strength g .

It is worth noting that the square lattice dispersion relation has a number of special features, such as a perfect nesting and a van-Hove singularity in the density of states (at half-filling), which lead to CDW order at weak electron-phonon coupling. For stronger coupling cases, the occurrence of CDW order is less dependent on the Fermi surface features, and its behavior on a square lattice is generic, e.g., with CDW transition temperatures being similar to those on other two-dimensional (2D) bipartite lattices [24–27]. In this work, we analyze both weak and strong coupling regimes at half-filling, $\langle n_{i\sigma} \rangle = 1/2$, which is obtained by fixing $\mu = -2g^2/\omega_0$, regardless of the lattice size or temperature, due to an appropriate particle-hole symmetry. We further set $t = 1$ to represent the unit of energy, and we use units where $\hbar = k_B = 1$. We also define $\lambda_D = g^2/(z t \omega_0)$ as the dimensionless electron-phonon coupling, where $z = 4$ is the coordination number for the square lattice. In what follows, we consider two cases: (i) the adiabatic case, with $\omega_0/t = 1/2$ and an intermediate coupling strength $\lambda_D = 1/2$ ($g = 1$); and (ii) the antiadiabatic case, with $\omega_0/t = 4$ and a weak coupling strength $\lambda_D = 1/4$ ($g = 2$).

Methods. We employ the determinant quantum Monte Carlo (DQMC) method [29–32], an unbiased auxiliary-field approach that provides finite-temperature properties of interacting fermions. Within this approach, both equal-time and unequal-time quantities can be calculated. See [28] for more details.

Charge modulations are probed by analyzing the density-density correlation functions $\langle n_i n_j \rangle$ and their Fourier transform, the charge structure factor

$$S(\mathbf{q}) = \frac{1}{N} \sum_{i,j} e^{i\mathbf{q}\cdot(\mathbf{r}_i - \mathbf{r}_j)} \langle n_i n_j \rangle, \quad (2)$$

where $N = L^2$ is the number of lattice sites in the system. Similarly, superconducting properties are examined by means of the s -wave pairing susceptibility,

$$\chi_s = \frac{1}{N} \int_0^\beta d\tau \langle \Delta(\tau) \Delta^\dagger(0) \rangle, \quad (3)$$

in which $\beta = 1/T$ is the inverse temperature and $\Delta(\tau) = \sum_i d_{i\downarrow}(\tau) d_{i\uparrow}(\tau)$, with $d_{i\sigma}(\tau) = e^{\tau\mathcal{H}} d_{i\sigma} e^{-\tau\mathcal{H}}$. Although the equal-time pairing correlations at large spatial separation can also be used to probe superconductivity, the full susceptibility provides a more sensitive measure, especially in the case of a Kosterlitz-Thouless transition, as is expected to occur in 2D lattices [31,43,44].

Finally, we investigate transport properties by calculating a proxy of the direct current (dc) conductivity [19,45]

$$\sigma_{dc} \approx \frac{\beta^2}{\pi} \Lambda_{xx}(\mathbf{q} = \mathbf{0}, \tau = \beta/2), \quad (4)$$

where $\Lambda_{xx}(\mathbf{q}, \tau) = \langle j_x(\mathbf{q}, \tau) j_x(-\mathbf{q}, 0) \rangle$ is the current-current correlation function, and $j_x(\mathbf{q}, \tau)$ is the Fourier transform of $j_x(\mathbf{r}, \tau) = -it (d_{\mathbf{r}+\hat{x},\sigma}^\dagger d_{\mathbf{r},\sigma} - d_{\mathbf{r},\sigma}^\dagger d_{\mathbf{r}+\hat{x},\sigma})(\tau)$. We carry out the

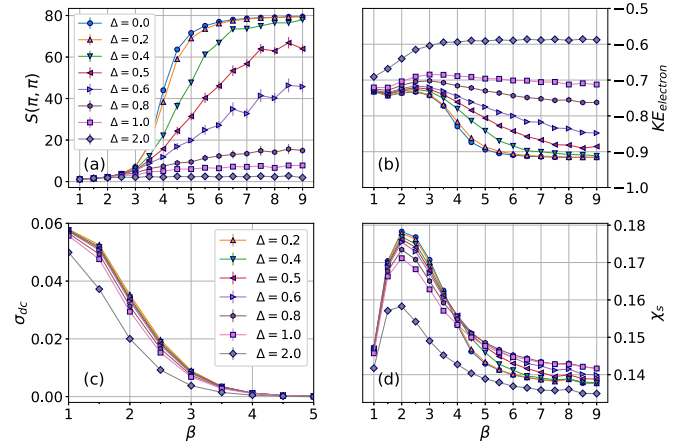


FIG. 1. (a) Charge structure factor, (b) kinetic energy of electrons, (c) dc conductivity, and (d) s -wave pair susceptibility as functions of the inverse temperature, and for different disorder strength, at fixed $L = 10$, $\omega_0 = 0.5$, and $\lambda_D = 0.5$ ($g = 1$). Results are shown for the dc conductivity only for larger Δ , where Eq. (4) is valid [45].

calculations on lattice sizes from 6×6 to 12×12 , and we average our expectation values over 110 disorder realizations.

Results. We first consider the response of charge modulations to disorder in the adiabatic case by fixing $\omega_0/t = 0.5$ and $\lambda_D = 1/2$ ($g = 1$). When $\Delta = 0$, there is a large enhancement of $S(\pi, \pi)$ around $\beta \approx 4$, as presented in Fig. 1(a), in line with recent studies [46,47] that show a CDW transition at $\beta_c = 4.1 \pm 0.1$ (see also the SM [28]). In the presence of weak disorder, $\Delta \lesssim 0.3t$, the behavior of $S(\pi, \pi)$ is only slightly changed from that of the clean system, suggesting the continued existence of long-range charge correlations over length scales up to the lattice sizes being simulated, as displayed in Fig. 1(a). However, as disorder increases further, $S(\pi, \pi)$ has its characteristic energy scale shifted to larger β (lower temperature), and its strength reduced. Eventually, for $\Delta \approx t$, long-range correlations seem entirely destroyed, even at very low temperatures.

At this point, it is convenient to estimate the size of Δ needed to break charge order. From a second-order perturbation theory [48], the effective attraction between electrons is given by $U_{\text{eff}} = -2g^2/\omega_0$, therefore the CDW scale may be estimated as $4t^2/|U_{\text{eff}}| = 2t^2\omega_0/g^2$. Given this, when Δ exceeds some fraction of this value, one should expect the charge correlations to be suppressed. Indeed, this yields $\Delta_c \lesssim 1$ for $\omega_0 = 0.5$, $g = 1$, in rough agreement with the vanishing of the CDW correlations for $\Delta \gtrsim 0.5$, displayed in Fig. 1(a).

Further insight into this crossover is provided by the behavior of the electronic kinetic energy, exhibited in Fig. 1(b). At weak disorder, despite the occurrence of a Peierls-like charge gap, the alternation of empty and doubly occupied sites associated with strong CDW correlations promotes charge fluctuations, and hence the magnitude of the kinetic energy increases as the temperature is lowered. By contrast, in the strong disordered case, the pairs are localized randomly, with some doublons at adjacent sites, precluding virtual hopping. As a consequence, the kinetic energy decreases in magnitude as $T \rightarrow 0$. Despite the suppression of the CDW order,

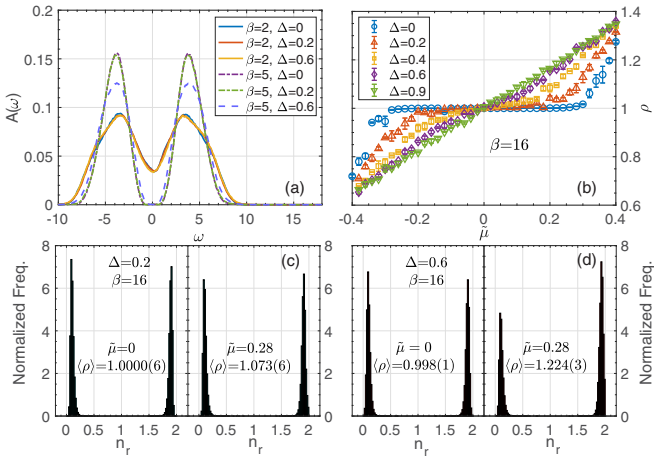


FIG. 2. (a) Density of states as a function of energy, (b) electron density, ρ , as a function of shifted chemical potential, $\tilde{\mu} = \mu + 2g^2/\omega_0$, and the electron distribution at half-filling (left) and away from half-filling (right) at fixed (c) $\Delta = 0.2$ and (d) $\Delta = 0.6$. $L = 10$, $\omega = 0.5$, and $\lambda_D = 0.5$ ($g = 1$).

Fig. 1(c) shows that the conductivity decreases as T is lowered, with $d\sigma_{dc}/dT > 0$, indicating an insulating behavior for all values of Δ . In line with this, the pairing susceptibility, shown in Fig. 1(d), remains small for all Δ , suggesting that local electron pairs are not correlated.

We now characterize in more detail the large Δ behavior. Figure 2(a) shows the spectral function $A(\omega)$, obtained via the analytic continuation of $G(\mathbf{q}, \tau) = \langle \mathcal{T} d(\mathbf{q}, \tau) d^\dagger(\mathbf{q}, 0) \rangle = \int_{-\infty}^{\infty} d\omega \frac{e^{-\tau\omega}}{1+e^{-\beta\omega}} A(\mathbf{q}, \omega)$, where \mathcal{T} is the imaginary time ordering operator, and $A(\omega)$ sums over all momenta; see, e.g., the SM [28]. The spectral weight at the Fermi level is suppressed at low T , with an opening of a single-particle gap. This occurs for both clean and disordered cases, even for large disorder, where the CDW has been completely destroyed, suggesting an insulating behavior for any disorder strength. Typically, the opening of such gaps in $A(\omega)$ is associated with a vanishing compressibility $\kappa = d\rho/d\mu$. This happens, e.g., in the half-filled fermionic Hubbard model, both in the weak-coupling Slater and strong-coupling Mott regimes. Similarly, in our disordered Holstein model, the compressibility also vanishes at weak disorder, as shown in Fig. 2(b). However, at large Δ , the gap in $A(\omega)$ is *not* accompanied by $\kappa = 0$. As displayed in Fig. 2(b), the plateau in $\rho(\mu)$ is substantially smeared at $\Delta/t \sim 0.4$, and completely destroyed at $\Delta/t \sim 0.6$.

In both band and Mott insulators, $A(\omega) = 0$ and $\kappa = 0$ go hand-in-hand. The unusual behavior whereby $A(\omega = 0) = 0$ but $\kappa \neq 0$ derives from the fact that the effective local attractive interaction, due to phonon modes, favors the addition of pairs of fermions to the system, while resisting the addition of individual ones. This picture is supported by analyzing the electron distribution on the lattice during the Monte Carlo simulations. In Figs. 2(c) and 2(d), histograms of the local density n_r are sharply peaked around 0 and 2 but not 1 for all disorder strengths, indicating that we mostly have doubly occupied or empty sites. Similar distributions are also observed away from half-filling. For instance, fixing

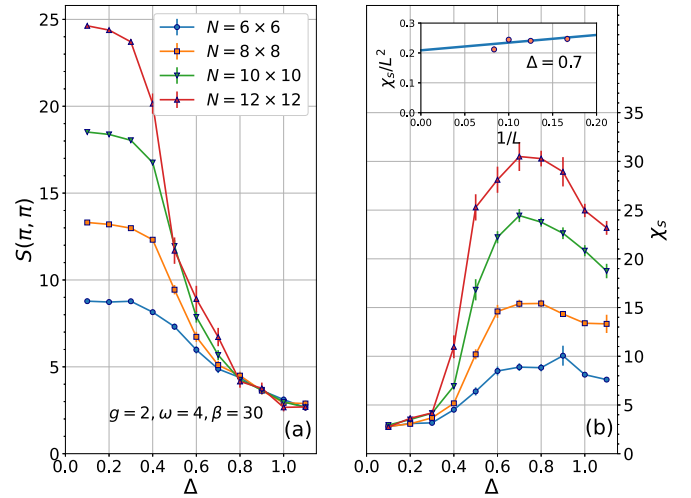


FIG. 3. (a) Charge structure factor $S(\pi, \pi)$, (b) s -wave pairing susceptibility χ_s as a function of disorder strength Δ , at fixed $\beta = 30$, $\omega_0 = 4$, and $\lambda_D = 1/4$ ($g = 2$). Inset: the normalized pairing susceptibility χ_s/L^2 as a function of $1/L$ at $\Delta = 0.7$.

$\tilde{\mu} = \mu + 2g^2/\omega_0 = 0.28$, and comparing the electron distribution at $\Delta/t = 0.2$ with $\Delta/t = 0.6$, the same chemical potential adds more pairs of electrons into the system and causes a more distinguished imbalance between empty and doubly occupied sites at larger disorder. This supports the picture that adding pairs of electrons is the mechanism by which the system responds to increasing μ . Unlike the repulsive Hubbard model, where the electron-electron interaction U favors moment formation (singly occupied sites) and the random site energies favor pairs, here the electron-phonon interaction, g , and Δ both promote binding. Together, the properties shown in Fig. 2 point to an insulating phase characterized by a gapless fermion pair excitation, but a gapped spectrum for single-particle ones.

We now discuss the antiadiabatic regime, fixing $\omega_0/t = 4$ and $\lambda_D = 1/4$ ($g = 2$). Figure 3(a) shows the evolution of $S(\pi, \pi)$ with disorder, at a fixed low temperature $T = t/30$. As in the adiabatic regime, increasing Δ strongly suppresses the charge response, destroying the CDW phase. However, in stark contrast with the former case, here the behavior of the pair susceptibility is dramatically different: χ_s is two orders of magnitude larger, and it exhibits a peak around $\Delta/t = 0.7$, as displayed in Fig. 3(b). The magnitudes of these charge structure factors and superconducting susceptibilities are consistent with those of their magnetic and pairing analogs indicating long-range order in the repulsive [49] and attractive Hubbard models [34,44,50]. Although these large values of χ_s are suggestive, finite-size scaling (FSS) is required to establish the nature of the phase. One approach to this FSS is to take data at very low temperatures, such as $T/t = 1/30$ in Fig. 3 so that one is essentially at $T = 0$, on the simulated lattice size for that value of randomness. The inset of Fig. 3(b) shows that χ_s/L^2 , at $\Delta/t = 0.7$, has a finite value when extrapolated to $L \rightarrow \infty$, corresponding to long-range order and a divergence of χ_{pairing} in the thermodynamic limit. The qualitative picture is that, for these parameters, disorder drives a SC state at

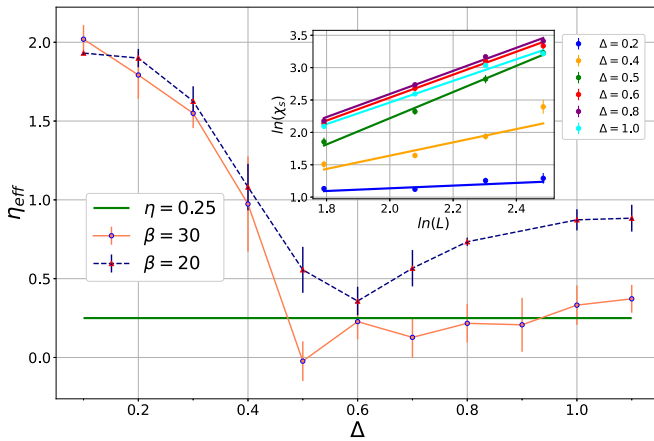


FIG. 4. The effective KT power law $\eta_{\text{eff}}(T)$ is shown as a function of disorder Δ for two fixed low temperatures. $\eta_{\text{eff}}(T) < 1/4$ for $T/t = 1/30$ in a range of intermediate Δ , suggesting a superconducting state.

commensurate filling as charge correlations are suppressed, and new energy states are created near the Fermi surface for pairing. Given this, the results of these QMC simulations are a crossover from a phase consisting of CDW-puddles to a SC ordered one.

A more refined FSS analysis proceeds as follows: We expect the 2D superconducting transition suggested by the data of Fig. 3 to be in the Kosterlitz-Thouless universality class. Thus the pair susceptibility $\chi_s \sim L^{2-\eta(T)}$ with a temperature-dependent exponent $\eta(T)$. At the KT transition point, $\eta(T_c) = 1/4$ and $\eta(T) \rightarrow 0$ in the ground state. Meanwhile, for $T > T_{\text{KT}}$, the pair correlations decay exponentially on sufficiently large lattices, therefore $\chi_s \sim L^0$ according to Eq. (3), i.e., $\eta = 2$. Figure 4 shows the results for such FSS analysis, in which we have used plots of $\ln(\chi_s)$ versus $\ln(L)$ to extract η_{eff} at the fixed temperatures $T/t = 1/20, 1/30$ of the simulations, as displayed in the inset. We refer to this as an “effective” η to acknowledge finite-size effects. The main panel of Fig. 4 shows η_{eff} at these two temperatures as a function of disorder Δ . At small Δ , deep in the CDW phase, pairing correlations decay rapidly and we see the expected $\eta_{\text{eff}} = 2$. For $T/t = 1/20$, η_{eff} comes down rapidly as disorder strength is increased, indicative of pairing correlations that are approaching the size of the lattice. However, η_{eff} still exceeds the universal KT value $\eta_{\text{eff}}(T_c) = 1/4$ for all Δ . There is no superconductivity at this temperature. For $T/t = 1/30$, on the other hand, $\eta_{\text{eff}} < 1/4$ in a range of intermediate Δ . In this window, $T = 1/30 < T_c$ and the system is in a superconducting phase. The error bars are conservatively estimated, and they represent a complex combination of statistical uncertainty for individual disorder realizations, the disorder averaging, and uncertainty associated with the FSS fit to extract η .

The overall picture that emerges from Figs. 3 and 4 is that substantial charge correlations are present at $T/t \lesssim 1/10$ in the weak disorder region, $\Delta/t \lesssim 0.5$, while a SC dome emerges for stronger disorder values at $T/t \lesssim 1/20$. The issue of how the CDW and SC phases meet at temperatures below $T = 0.033$ is beyond the scope of the present set of simulations. The heat maps of Fig. S1 of the SM [28] suggest that there is a narrow region where both $S(\pi, \pi)$ and χ_s are large.

However, while we are able to perform definitive FSS analysis within the individual CDW and SC phases, the corresponding data at the interface between them do not provide an unambiguous conclusion. Furthermore, the coupling of random fields to the CDW order parameter prevents the occurrence of true diagonal long-range order [11]. Notwithstanding, the emergence of SC is allowed in the ground state, as indicated by our FSS analysis, and also emphasized in the heat map presented in the SM [28].

Concluding remarks. Although the two parameter regimes for which we have presented results are distinguished by the value of ω_0/t , we believe the qualitative explanation for the difference in behavior, i.e., the presence of an intermediate SC phase, lies in the fact that the former corresponds to intermediate and the latter to weak dimensionless coupling. For strong and intermediate couplings, the composite electron-phonon polarons are small, and hence easily localized by disorder. At weak dimensionless coupling, the polarons are much larger, and the disorder potential is therefore to some extent averaged out over their volume. Thus, after Δ destroys the CDW, it does not yet localize the pairs, which remain mobile and condense into a SC phase.

Tuning between CDW and paired phases can be accomplished via pressure or doping, and it is a phenomenon that has also been extensively explored experimentally. Analogies between antiferromagnetic-SC and CDW-SC phases have also been remarked [30,51]. However, the latter transition has received much less attention from the QMC community. Early work on the doping-driven CDW-SC transition in the Holstein model [52,53] has been extended to transitions at commensurate filling caused by the introduction of band dispersion [54], and a comparison with Migdal-Eliashberg theory [55]. Additional QMC literature has also considered the interplay between electron-electron and electron-phonon interactions, as in the Hubbard-Holstein model [56–61].

This paper has described a detailed QMC study of the effect of disorder on the CDW transition, and it has shown that, in certain parameter regimes, randomness can give rise to a SC state. Earlier work has suggested that the electron-phonon coupling can renormalize the disorder potentials, leading to a ground state that may not exhibit Anderson localization [62–65]. The present study suggests an even more subtle consequence of the disorder-interaction interplay, namely the emergence of off-diagonal ordered phases from diagonal disorder at commensurate filling.

We expect our results to apply quite generally to the Holstein model on other bipartite geometries (e.g., 3D cubic) where CDW order is dominant at half-filling [25,26,61]. The honeycomb lattice might be particularly interesting to investigate, since it has a quantum critical point for couplings below which CDW order is absent. SC might still emerge with added disorder in this semimetallic regime from the filling up of the density of states, which vanishes linearly in the clean limit. We also expect our results to apply generally to different choices of λ , ω_0 which have the same λ_D [66]. In the clean case, the CDW transition temperature has recently been found as a function of λ_D [24–26], a feature whose behavior with randomness would be interesting to examine in future work.

Acknowledgments. The work of B.X. and R.T.S. was supported by Grant No. DE-SC0014671 funded by the US Department of Energy, Office of Science. N.C.C. was partially supported by the Brazilian funding agencies CAPES and CNPq, and he also acknowledges PRACE for awarding him access to Marconi at CINECA, Italy (PRACE-2019204934).

E.K. acknowledges support from the National Science Foundation under Grant No. DMR-1918572. G.G.B. acknowledges support from the University of the Côte d'Azur IDEX Jedi and Beijing CSRC. Computations were performed on the Spartan facility supported by NSF OAC-162664 at SJSU.

- [1] E. Abrahams, P. W. Anderson, D. C. Licciardello, and T. V. Ramakrishnan, Scaling Theory of Localization: Absence of Quantum Diffusion in Two Dimensions, *Phys. Rev. Lett.* **42**, 673 (1979).
- [2] F. Wegner, Inverse participation ratio in $2 + \epsilon$ dimensions, *Z. Phys. B* **36**, 209 (1980).
- [3] K. B. Efetov, A. I. Larkin, and D. E. Khmel'nitskii, Interaction of diffusion modes in the theory of localization, *Zh. Eksp. Teor. Fiz.* **79**, 1120 (1980) [*Sov. Phys. JETP* **52**, 568 (1980)].
- [4] P. A. Lee and T. V. Ramakrishnan, Disordered electronic systems, *Rev. Mod. Phys.* **57**, 287 (1985).
- [5] T. Giamarchi and H. J. Schulz, Anderson localization and interactions in one-dimensional metals, *Phys. Rev. B* **37**, 325 (1988).
- [6] D. Belitz and T. R. Kirkpatrick, The Anderson-Mott transition, *Rev. Mod. Phys.* **66**, 261 (1994).
- [7] E. Dagotto, Complexity in strongly correlated electronic systems, *Science* **309**, 257 (2005).
- [8] A. V. Balatsky, I. Vekhter, and J.-X. Zhu, Impurity-induced states in conventional and unconventional superconductors, *Rev. Mod. Phys.* **78**, 373 (2006).
- [9] E. Abrahams, *50 Years of Anderson Localization* (World Scientific, Singapore, 2010).
- [10] V. Dobrosavljević, N. Trivedi, and J. M. Valles Jr., *Conductor-insulator Quantum Phase Transitions* (Oxford University Press, Oxford, UK, 2012).
- [11] T. Vojta, Disorder in quantum many-body systems, *Annu. Rev. Condens. Matter Phys.* **10**, 233 (2019).
- [12] S. V. Kravchenko and M. P. Sarachik, Metal-insulator transition in two-dimensional electron systems, *Rep. Prog. Phys.* **67**, 1 (2003).
- [13] A. M. Lobos, R. M. Lutchyn, and S. Das Sarma, Interplay of Disorder and Interaction in Majorana Quantum Wires, *Phys. Rev. Lett.* **109**, 146403 (2012).
- [14] A. Krishna, M. Ippoliti, and R. N. Bhatt, Localization and interactions in topological and nontopological bands in two dimensions, *Phys. Rev. B* **100**, 054202 (2019).
- [15] S. S. Kondov, W. R. McGehee, J. J. Zirbel, and B. DeMarco, Three-dimensional anderson localization of ultracold matter, *Science* **334**, 66 (2011).
- [16] D. M. Basko, I. L. Aleiner, and B. L. Altshuler, *Ann. Phys. (NY)* **321**, 1126 (2006).
- [17] R. Nandkishore and D. A. Huse, *Annu. Rev. Condens. Matter Phys.* **6**, 15 (2015).
- [18] Y. B. Lev, G. Cohen, and D. R. Reichman, *Phys. Rev. Lett.* **114**, 100601 (2015).
- [19] P. J. H. Denteneer, R. T. Scalettar, and N. Trivedi, Conducting phase in the two-dimensional disordered Hubbard model, *Phys. Rev. Lett.* **83**, 4610 (1999).
- [20] H. Terletska, Y. Zhang, K.-M. Tam, T. Berlijn, L. Chioncel, N. S. Vidhyadhiraja, and M. Jarrell, Systematic quantum cluster typical medium method for the study of localization in strongly disordered electronic systems, *Appl. Sci.* **8**, 2401 (2018).
- [21] E. Y. Loh, J. E. Gubernatis, R. T. Scalettar, S. R. White, D. J. Scalapino, and R. L. Sugar, Sign problem in the numerical simulation of many-electron systems, *Phys. Rev. B* **41**, 9301 (1990).
- [22] M. Troyer and U.-J. Wiese, Computational Complexity and Fundamental Limitations to Fermionic Quantum Monte Carlo Simulations, *Phys. Rev. Lett.* **94**, 170201 (2005).
- [23] V. I. Iglovikov, E. Khatami, and R. T. Scalettar, Geometry dependence of the sign problem in quantum Monte Carlo simulations, *Phys. Rev. B* **92**, 045110 (2015).
- [24] M. Weber and M. Hohenadler, Two-dimensional Holstein-Hubbard model: Critical temperature, Ising universality, and bipolaron liquid, *Phys. Rev. B* **98**, 085405 (2018).
- [25] Y.-X. Zhang, W.-T. Chiu, N. C. Costa, G. G. Batrouni, and R. T. Scalettar, Charge order in the Holstein model on a Honeycomb lattice, *Phys. Rev. Lett.* **122**, 077602 (2019).
- [26] C. Chen, X. Y. Xu, Zi. Y. Meng, and M. Hohenadler, Charge-Density-Wave Transitions of Dirac Fermions Coupled to Phonons, *Phys. Rev. Lett.* **122**, 077601 (2019).
- [27] B. Cohen-Stead, K. Barros, ZY Meng, C. Chen, R. T. Scalettar, and G. G. Batrouni, Langevin simulations of the half-filled cubic Holstein model, *Phys. Rev. B* **102**, 161108(R) (2020).
- [28] See Supplemental Material at <http://link.aps.org/supplemental/10.1103/PhysRevB.103.L060501> for more details about the CDW-SC competition in the antiadiabatic limit, the determinant Quantum Monte Carlo method, CDW transition in the clean limit, specific heat, temperature dependence in the antiadiabatic limit, and disorder dependence in the adiabatic limit, which includes Refs. [29–42].
- [29] R. Blankenbecler, D. J. Scalapino, and R. L. Sugar, Monte Carlo calculations of coupled boson-fermion systems. I, *Phys. Rev. D* **24**, 2278 (1981).
- [30] R. T. Scalettar, N. E. Bickers, and D. J. Scalapino, Competition of pairing and Peierls-charge-density-wave correlations in a two-dimensional electron-phonon model, *Phys. Rev. B* **40**, 197 (1989).
- [31] R. M. Noack, D. J. Scalapino, and R. T. Scalettar, Charge-Density-Wave and Pairing Susceptibilities in a Two-Dimensional Electron-Phonon Model, *Phys. Rev. Lett.* **66**, 778 (1991).
- [32] R. R. dos Santos, Introduction to quantum Monte Carlo simulations for fermionic systems, *Braz. J. Phys.* **33**, 36 (2003).
- [33] M. Hohenadler and G. G. Batrouni, Dominant charge-density-wave correlations in the Holstein model on the half-filled square lattice, *Phys. Rev. B* **100**, 165114 (2019).
- [34] K. Bouadim, Y. L. Loh, M. Randeria, and N. Trivedi, Single- and two-particle energy gaps across the disorder-driven superconductor-insulator transition, *Nat. Phys.* **7**, 884 (2011).

- [35] A. McMahan, C. Huscroft, R. T. Scalettar, and E. L. Pollock, Volume collapse transitions in the rare earth metals, *J. Comp.-Aided Mater. Des.* **5**, 131 (1998).
- [36] T. Paiva, R. T. Scalettar, C. Huscroft, and A. K. McMahan, Signatures of spin and charge energy scales in the local moment and specific heat of the half-filled two-dimensional Hubbard model, *Phys. Rev. B* **63**, 125116 (2001).
- [37] M. Ulmke and R. T. Scalettar, Magnetic correlations in the two dimensional Anderson-Hubbard model, *Phys. Rev. B* **55**, 4149 (1997).
- [38] M. Ulmke, V. Janiš, and D. Vollhardt, Anderson-Hubbard model in infinite dimensions, *Phys. Rev. B* **51**, 10411 (1995).
- [39] R. N. Silver, D. S. Sivia, and J. E. Gubernatis, Maximum-entropy method for analytic continuation of quantum Monte Carlo data, *Phys. Rev. B* **41**, 2380 (1990).
- [40] J. E. Gubernatis, M. Jarrell, R. N. Silver, and D. S. Sivia, Quantum Monte Carlo simulations and maximum entropy: Dynamics from imaginary-time data, *Phys. Rev. B* **44**, 6011 (1991).
- [41] A. W. Sandvik, Stochastic method for analytic continuation of quantum Monte Carlo data, *Phys. Rev. B* **57**, 10287 (1998).
- [42] N. E. Bickers, D. J. Scalapino, and R. T. Scalettar, Cdw and sdw mediated pairing mechanisms, *Int. J. Mod. Phys. B* **1**, 687 (1987).
- [43] C. Huscroft and R. T. Scalettar, Effect of disorder on charge-density wave and superconducting order in the half-filled attractive Hubbard model, *Phys. Rev. B* **55**, 1185 (1997).
- [44] T. Paiva, R. R. dos Santos, R. T. Scalettar, and P. J. H. Denteneer, Critical temperature for the two-dimensional attractive Hubbard model, *Phys. Rev. B* **69**, 184501 (2004).
- [45] N. Trivedi, R. T. Scalettar, and M. Randeria, Superconductor-insulator transition in a disordered electronic system, *Phys. Rev. B* **54**, R3756 (1996).
- [46] C. Chen, X. Y. Xu, J. Liu, G. Batrouni, R. Scalettar, and Z. Y. Meng, Symmetry-enforced self-learning Monte Carlo method applied to the Holstein model, *Phys. Rev. B* **98**, 041102(R) (2018).
- [47] S. Li, P. M. Dee, E. Khatami, and S. Johnston, Accelerating lattice quantum Monte Carlo simulations using artificial neural networks: Application to the Holstein model, *Phys. Rev. B* **100**, 020302(R) (2019).
- [48] E. Berger, P. Valášek, and W. von der Linden, Two-dimensional Hubbard-Holstein model, *Phys. Rev. B* **52**, 4806 (1995).
- [49] C. N. Varney, C. R. Lee, Z. J. Bai, S. Chiesa, M. Jarrell, and R. T. Scalettar, Quantum Monte Carlo study of the 2D fermion Hubbard model at half-filling, *Phys. Rev. B* **80**, 075116 (2009).
- [50] R. T. Scalettar, E. Y. Loh, J. E. Gubernatis, A. Moreo, S. R. White, D. J. Scalapino, R. L. Sugar, and E. Dagotto, Phase Diagram of the Two-Dimensional Negative U Hubbard Model, *Phys. Rev. Lett.* **62**, 1407 (1989).
- [51] I. Esterlis, S. Kivelson, and D. Scalapino, A bound on the superconducting transition temperature, *Nat. Phys. J., Quantum Mater.* **3**, 59 (2018).
- [52] M. Vekić, R. M. Noack, and S. R. White, Charge-density waves versus superconductivity in the Holstein model with next-nearest-neighbor hopping, *Phys. Rev. B* **46**, 271 (1992).
- [53] J. K. Freericks, M. Jarrell, and D. J. Scalapino, Holstein model in infinite dimensions, *Phys. Rev. B* **48**, 6302 (1993).
- [54] N. C. Costa, T. Blommel, W.-T. Chiu, G. Batrouni, and R. T. Scalettar, Phonon Dispersion and the Competition Between Pairing and Charge Order, *Phys. Rev. Lett.* **120**, 187003 (2018).
- [55] I. Esterlis, B. Nosarzewski, E. W. Huang, B. Moritz, T. P. Devereaux, D. J. Scalapino, and S. A. Kivelson, Breakdown of the Migdal-Eliashberg theory: A determinant quantum Monte Carlo study, *Phys. Rev. B* **97**, 140501(R) (2018).
- [56] S. Yamazaki, S. Hoshino, and Y. Kuramoto, Continuous-time quantum Monte Carlo study of strong coupling superconductivity in Holstein-Hubbard model, *JPS Conf. Proc.* **3**, 016021 (2014).
- [57] S. Karakuzu, L. F. Tocchio, S. Sorella, and F. Becca, Superconductivity, charge-density waves, antiferromagnetism, and phase separation in the Hubbard-Holstein model, *Phys. Rev. B* **96**, 205145 (2017).
- [58] T. Ohgoe and M. Imada, Competition Among Superconducting, Antiferromagnetic, and Charge Orders with Intervention by Phase Separation in the 2D Holstein-Hubbard Model, *Phys. Rev. Lett.* **119**, 197001 (2017).
- [59] N. C. Costa, K. Seki, S. Yunoki, and S. Sorella, Phase diagram of the two-dimensional Hubbard-Holstein model, *Commun. Phys.* **3**, 1 (2020).
- [60] Y. Wang, I. Esterlis, T. Shi, J. I. Cirac, and E. Demler, Zero-temperature phases of the two-dimensional Hubbard-Holstein model: A non-Gaussian exact diagonalization study, *Phys. Rev. Res.* **2**, 043258 (2020).
- [61] N. C. Costa, K. Seki, and S. Sorella, Magnetism and charge order in the honeycomb lattice, *arXiv:2009.05586*.
- [62] F. X. Bronold and H. Fehske, Anderson localization of polaron states, *Phys. Rev. B* **66**, 073102 (2002).
- [63] H. Ebrahimnejad and M. Berciu, Perturbational study of the lifetime of a Holstein polaron in the presence of weak disorder, *Phys. Rev. B* **86**, 205109 (2012).
- [64] H. Ebrahimnejad and M. Berciu, Trapping of three-dimensional Holstein polarons by various impurities, *Phys. Rev. B* **85**, 165117 (2012).
- [65] O. R. Tozer and W. Barford, Localization of large polarons in the disordered Holstein model, *Phys. Rev. B* **89**, 155434 (2014).
- [66] Y. Zhang, C. Feng, G. Batrouni, and R. Scalettar (unpublished).